Article

Effect of Sintering Temperature on the Physical and Mechanical Characteristics of Fabricated ZrO2-Cr-Ni-Ce-Y Composite

Brajesh Chandra Saini , Naman Jain , Dinesh Kumar Rao , Varun Singhal , Akarsh Verma , Dayanand M. Goudar , K Raju * , Deesy G. Pinto *

Posted Date: 9 September 2024

doi: 10.20944/preprints202409.0398.v1

Keywords: powder metallurgy; microhardness; flexural strength; zirconium dioxide; sintering

Article

Effect of Sintering Temperature on the Physical and Mechanical Characteristics of Fabricated ZrO2-Cr-Ni-Ce-Y Composite

Brajesh Chandra Saini [1], Naman Jain [2], Dinesh Kumar Rao [1], Varun Singhal [3], Akarsh Verma [4], Dayanand M Goudar [5], K. Raju [6,*] and Deesy G. Pinto [7,8,*]

[1] Department of Mechanical Engineering, Dr. Ram Manohar Lohia Avadh University Faizabad, Ayodhya, 224001, India
[2] Department of Mechanical Engineering, ABES Engineering College, Ghaziabad, 201009, India
[3] Department of Mechanical Engineering, GLA University, Mathura, 281406, India
[4] Department of Mechanical Engineering, University of Petroleum and Energy Studies, Dehradun, 248007, India
[5] Department of Mechanical Engineering, Tontadarya College of Engineering, Gadag – 582101, India
[6] Department of Mechanical Engineering, St Joseph Engineering College, Mangaluru – 575028, India
[7] Department of Civil Engineering & Geology, University of Madeira, Campus da Penteada, 9020-105 Funchal, Portugal
[8] Departament of Civil Engineering & Architecture, Faculty of Engineering, University of Beira Interior, Covilhã, Portugal
* Correspondence: rajuk@sjec.ac.in, deesy.pinto@staff.uma.pt

Abstract: This study investigates the synthesis and characterization of zirconium oxide (ZrO_2)-based metal-composites doped with cerium (Ce) and yttrium (Y), using chromium (Cr) and nickel (Ni) as base metals. These constituents were selected for their superior mechanical properties and compatibility with the ceramic phase. High-purity powders were homogenized via high-energy ball milling, followed by cold isostatic pressing (CIP) and sintering in a controlled atmosphere. The sintering process was conducted at various temperatures (850°C to 1350°C) to examine densification, grain growth, and microstructure evolution. Scanning Electron Microscopy (SEM) revealed a homogeneous distribution of phases, with distinct microstructural features attributed to each element at different sintering temperatures. Density measurements using the water immersion method and theoretical calculations demonstrated increased density and reduced porosity with higher sintering temperatures. Vickers hardness testing indicated that hardness improved with increased sintering temperature, peaking around 1150°C due to cerium and yttrium reinforcement within the matrix. Flexural strength tests showed the highest value at 1350°C, with a significant drop in porosity, suggesting enhanced mechanical properties due to efficient doping and phase transformations. Overall, the incorporation of cerium and yttrium significantly improved the mechanical behavior and phase stability of the ZrO_2-Cr-Ni composites, highlighting their potential for advanced engineering applications.

Keywords: powder metallurgy; microhardness; flexural strength; zirconium dioxide; sintering

1. Introduction

In the realm of advanced materials, the quest for novel compositions and fabrication methods has driven researchers to explore uncharted territories, seeking materials that exhibit remarkable mechanical properties and diverse functionalities. The mixing of metals and ceramics has been a focal point of this pursuit, yielding composites that combine the best of both worlds: the toughness of metals and the hardness of ceramics. Among these innovative combinations, ZrO_2-Cr-Ni based metal-ceramic blends with yttrium (Y) and cerium (Ce), synthesized through the versatile technique of powder metallurgy, have emerged as a captivating subject of study. The union of ZrO_2, Cr, and Ni brings forth a triad of elements that encompass intriguing mechanical attributes. Zirconia (ZrO_2), a well-recognized ceramic, exhibits a rare phenomenon known as transformation toughening, wherein

 doi:10.20944/preprints202409.0398.v1

it undergoes a phase transition under mechanical stress, effectively retarding crack propagation. Chromium (Cr), on the other hand, introduces corrosion resistance and oxidation stability, characteristics particularly attractive for applications in demanding environments. Nickel (Ni), with its exceptional ductility and thermal conductivity, complements this amalgamation by enhancing the overall toughness and thermal performance. The addition of chromium (Cr) and nickel (Ni) to ZrO_2 has been shown to improve mechanical properties, but recent research has pushed the boundaries further by incorporating yttrium and cerium as reinforcing agents, giving rise to ZrO_2-Cr-Ni based metal-ceramic blends. Zhang et al. (2019) ventured into the nuances of phase transformations, elucidating the impact of yttrium on the martensitic transformation of ZrO_2, a phenomenon central to its transformation toughening mechanism [1]. This intricate dance of phases was further deciphered by Li et al. (2020), who unveiled the role of cerium in influencing the kinetics of phase transitions and crystallite growth [2]. For instance, Sun et al. (2019) investigated the effects of yttrium oxide (Y_2O_3) on the mechanical properties of alumina-zirconia composites [3]. The addition of Y_2O_3 was found to enhance the strength and toughness of the composites, attributed to the formation of a fine-grained microstructure and phase transformation toughening. Similarly, Wu et al. (2020) examined the role of cerium oxide (CeO_2) as a sintering aid in zirconia ceramics. The inclusion of CeO_2 promoted densification and grain growth, resulting in improved mechanical properties [4]. Zhu et al. (2018) [2] investigated the fracture toughness of ZrO_2-Cr-Ni-Y-Ce composites and observed significant enhancement compared to the pure ZrO_2 matrix [5]. The researchers attributed these enhancements to the formation of yttrium-stabilized tetragonal zirconia phases, which transformed into monoclinic zirconia under stress, effectively impeding crack propagation. In a comprehensive study by Chen et al. (2020), cerium additions were found to increase the fracture toughness of alumina ceramics, a phenomenon attributed to the formation of cerium oxide precipitates at grain boundaries [6]. This intriguing phenomenon, coupled with the notable ability of cerium to scavenge oxygen vacancies, holds great promise in the context of metal-ceramic composites. The symphony of mechanical attributes resonates through the resonance of these blends, encompassing parameters such as fracture toughness, fatigue resistance, and wear behaviour. The stage on which these compositions perform spans the spectrum of biomedical applications, where materials are thrust into the crucible of human well-being. Dental implants, bearing the weight of mastication, find their resonance in the enhanced mechanical stability of these metal-ceramic blends. Orthopaedic implants, bridging the chasm of bone fractures, draw strength from the augmented load-bearing capacity of these composites. The biomedical orchestra extends further to include prosthetic components, surgical instruments, and drug delivery systems, all harmonizing to the tune of enhanced mechanical functionality. The mechanical behaviour of ZrO_2-Cr-Ni based metal-ceramic blends with yttrium (Y) and cerium (Ce) prepared through powder metallurgy has emerged as a topic of significant interest in materials science and engineering. This literature review aims to explore the current state of research and advancements in this area, shedding light on the synthesis, mechanical properties, microstructural characteristics, and potential applications of these composites. Chen et al. (2020) investigated the impact of cerium additions on the fracture toughness of alumina ceramics. The researchers observed an increase in fracture toughness due to the formation of cerium oxide precipitates at grain boundaries, effectively hindering crack propagation [7]. Lee et al. (2019) employed powder metallurgy to fabricate ZrO_2-Cr-Ni based metal-ceramic blends with yttrium and cerium. The study demonstrated the feasibility of the PM route in obtaining uniform distribution of Y and Ce within the matrix, leading to improved mechanical properties [8]. A key advantage of PM is the ability to tailor the composition and microstructure of the composites by controlling powder characteristics, mixing parameters, and sintering conditions. Several studies have explored the influence of powder characteristics, such as particle size and morphology, on the mechanical properties of the resulting composites (Chang et al., 2019) [9]. Saito et al. (2016) demonstrated that the addition of Y promoted the formation of a tetragonal zirconia phase in alumina-zirconia composites, imparting transformation toughening capabilities and mitigating crack propagation [10]. Wang et al. (2017) [11] demonstrated the successful fabrication of Y_2O_3 and CeO_2 doped ZrO_2-Cr-Ni powders through co-precipitation and subsequent reduction processes. The addition of Y and Ce was found to enhance the sinter ability of the powders, resulting in denser and more homogenous compacts. Moreover, the unique mechanical behaviour of zirconia, such as transformation toughening, was further enhanced by yttrium additions. Cui et al. (2019) [12] elucidated the

 doi:10.20944/preprints202409.0398.v1

toughening mechanisms in ZrO_2-Cr-Ni based composites with yttrium, showing that the transformation from the tetragonal to the monoclinic phase under stress effectively hindered crack propagation, leading to improved fracture toughness. Tensile tests have been conducted to assess the mechanical strength and ductility of the composites (Li et al., 2019). The addition of yttrium and cerium has been shown to improve the tensile strength and elongation of the composites [13]. Hardness measurements are another essential aspect of the mechanical characterization, as hardness directly influences the wear resistance and load-bearing capacity of the materials. The incorporation of yttrium and cerium has been reported to enhance the hardness of the composites due to the formation of solid solutions and grain boundary strengthening (Miao et al., 2022) [14].

The aim of present investigation is to systematically examine the correlation between sintering temperature and the resulting physical and mechanical properties of a ZrO2-Cr-Ni-Ce-Y composite material. By subjecting fabricated samples to a range of sintering temperatures, the research aims to elucidate the optimal temperature for achieving desired mechanical characteristics. Understanding how sintering temperature affects the properties of ZrO2-Cr-Ni-Ce-Y composites can lead to the production of materials with superior mechanical characteristics. This research provides valuable insights into the microstructural evolution of ZrO2-based composites during sintering. ZrO2-based composites are widely used in various high-tech applications, including aerospace, automotive, and biomedical fields. Enhancing their properties through precise control of sintering parameters can expand their applicability and performance in these demanding environments.

2. Materials and Methods

Zirconium oxide (ZrO_2), chromium (Cr), and nickel (Ni) were chosen as the base metallic constituents due to their better tensile mechanical properties and compatibility with the ceramic phase. Yttrium powder (Y) and cerium powder (Ce) were selected as dopants for the ceramic phase based on their ability to improve mechanical performance and phase stability [15]. High-purity zirconium dioxide (ZrO_2), chromium (Cr), nickel (Ni), and yttrium (Y) powders from suppliers as shown in Table 1 were used for this procedure. The reason behind the selection of these materials was based on the theory of atomic radius of these elements. These all elements have almost very similar or less differences in their atomic radius, which would be an approval factor in the selection of appropriate matrix for this metal-composite. Also, the dopants used for this composite have compatible atomic sizes to be fitted perfectly in the lattice spaces of the metal-composites [16].

To prepare the composite specific volume percentages of each component are as follows: 20% ZrO_2, 35% Cr, 35% Ni, 5% Cerium, and 5% Yttrium. Afterward the powders were mixed and homogenized using a high-energy ball milling in the depressurized steel chamber to ensure a uniform distribution of the dopants i.e., Cerium and Yttrium within the ZrO_2-Cr-Ni matrix. Before compaction process the composite was mixed with the binding agent. Iso-Propyl alcohol of concentration 90-95% was used for obtaining a well compacted and matrixed product. The homogenized powder blend was compacted into green bodies using a cold isostatic press (CIP), with the compaction pressure and dwell time optimized to achieve the desired density and eliminate any defects in the green bodies. The composite samples raw powders were mixed separately using a high-energy ball mill to achieve a sustainable powder blend. The mixed samples powder was transferred to a die set for compaction. A punch of Ø6 mm was used in compaction. Under controlled pressure and through CIP the powder mixtures were compacted. The pressure applied during CIP from 130 MPa to 660 MPa to achieve the desired density and compaction of the powders. The pressing time depends on the equipment, the density requirements, and the properties of the powders. The pressing time for CIP was taken around 11 to 13 minutes. It was performed at room temperature to avoid sintering or densification due to heat. Therefore, the temperature was kept at or close to room temperature during the pressing process. A controlled and gradual pressurization is often employed to prevent sudden pressure fluctuations and ensure uniform compaction. A depressurization rate of 174 MPa per minute was employed in CIP.

Table 1. The details of the procured raw material.

Preprints.org (www.preprints.org) | NOT PEER-REVIEWED | Posted: 9 September 2024 doi:10.20944/preprints202409.0398.v1

Powder	Supplier	Purity (%)	Particle size (μm)	Apparent Density (g/cm³)	Density (ϱ) (g/cm³)
ZrO2	Sood Chemicals	95.01	1-5	5.5	5.89
Cr	Sood Chemicals	95.16	1-5	7.10	7.19
Ni	Sood Chemicals	95.10	1-5	8.02	8.91
Yttrium (Y)	Nano laboratories	98.20	1-5	4.4	6.96
Cerium (Ce)	Nano Laboratories	99.02	40	6.23	6.77

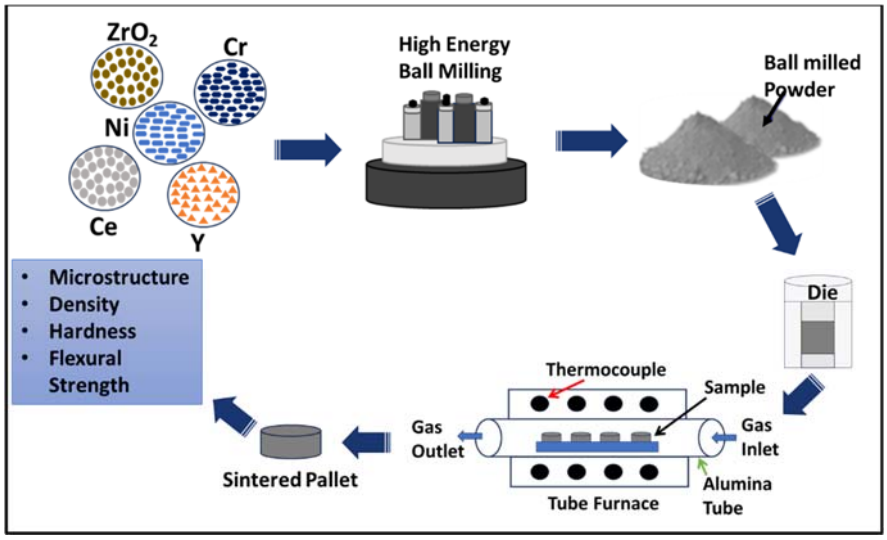

Figure 1. Steps followed in the production of ZrO_2-Cr-Ni-Ce-Y composites.

After that green bodies were sintered in a controlled atmosphere at specific temperature and duration. The sintering process is critical for promoting densification, grain growth control, and the formation of the desired microstructure in the composites. During sintering the temperature is critical parameter that determines the level of densification, grain growth control, the formation of the desired microstructure in the composites and the final mechanical properties of the sample. The compacted metal-composites were sintered at 1350°C for 3 hours 23 minutes. However, a keen record has been maintained by observing the sample at different temperatures i.e., at 850°C, 950°C, 1050°C, 1150°C, 1250°C and 1350°C. A controlled and gradual heating rate of 5.5°C per minute was employed to minimize thermal stresses and prevent cracking. The holding time i.e., 3 hours and 23 minutes was employed during sintering which allows sufficient densification and bonding between the powder particles. After the sintering, a controlled cooling rate like the heating rate was employed to avoid rapid thermal gradients and reduce the risk of cracking. During sintering of metal-based composites, a reducing atmosphere constituting hydrogen gas was prepared in the furnace to prevent oxidation and achieving better results. Figure 1 shows a graphical illustration of the composite fabrication procedure.

3. Characterization and Testing technique

3.1. SEM Analysis

SEM was used to examine the microstructure of the sintered samples. During preparing for scanning the sample 7.03mm x Ø7mm was decarbonated with the help of dry hot compressed air for

 doi:10.20944/preprints202409.0398.v1

removing the intact of Iso-propyl alcohol which was used as the binding medium in the powder metallurgy process. This decarbonization process will gives us more accurate results for SEM.

3.2. Density:

The water immersion method was utilized to determine the density of every sintered sample. The following mathematical relation was used to achieve the calculation:

$$\boldsymbol{\rho}_{ex} = \frac{W_a}{W_a - W_w} \quad (1)$$

ϱ_{ex}: Density of Sintered Sample
W_a: Weight in air
W_w: Weight in water
The rule of mixtures was utilized to compute the theoretical density of each fabricated composite. The inverse rule of mixtures is expressed as follows:

$$\frac{W}{\rho_{th}} = \left(\frac{W}{\rho}\right)_{ZrO2} + \left(\frac{W}{\rho}\right)_{Cr} + \left(\frac{W}{\rho}\right)_{Ni} + \left(\frac{W}{\rho}\right)_{Y} + \left(\frac{W}{\rho}\right)_{Ce} \quad (2)$$

3.3. Mechanical testing:

The polished sintered samples were used for bulk hardness testing. To ensure accuracy, at least five indentations were made on each sample, and the average hardness was calculated. Vickers hardness was measured using a microhardness tester. Indentations were made on the surface of the sintered samples. The 50mm x Ø7mm size of sample was grinded and polished to transform into a cuboidal shaped of dimension "29.86mm x 4.95mm x 4.95mm" to calculate hardness. Sintered sample was pieced into smaller sections with an aid of diamond saw in the dimensions of 10.37mm x Ø7mm. The three-point tensile tester machine is used for conducting flexural strength test. The flexural strength of the sintered samples was determined using a universal testing machine. Cylindrical samples were loaded axially until failure, and the maximum applied load were recorded to calculate the flexural strength.

3. Results and Discussion

3.1. Microstructural Analysis

The representative SEM micrograph of the sintered composite in Figure 2. Notably, it revealed a homogeneous distribution of ZrO_2, Cr, Ni, Ce, and Y phases across various sintering temperatures, indicating the effectiveness of the fabrication process. Within the microstructure, grey, black spot, greyish-white, polar white, and silverish white. The greyish areas were attributed to the presence of the Ni BCC phase, while black spots indicated the Cr FCC phase, and white spots represented the ZrO_2 phase. Additionally, the polar white cotton-shaped structures suggested the presence of yttrium, whereas the silverish white coloration depicted the presence of cerium in the metal-composite. At a sintering temperature of 850 °C, the formation of stone-shaped structures occurred, attributed to the slow fusion rate of Ni and Cr into ZrO_2, likely influenced by the addition of cerium and yttrium. This phase persisted up to a sintering temperature of 950 °C.

 doi:10.20944/preprints202409.0398.v1

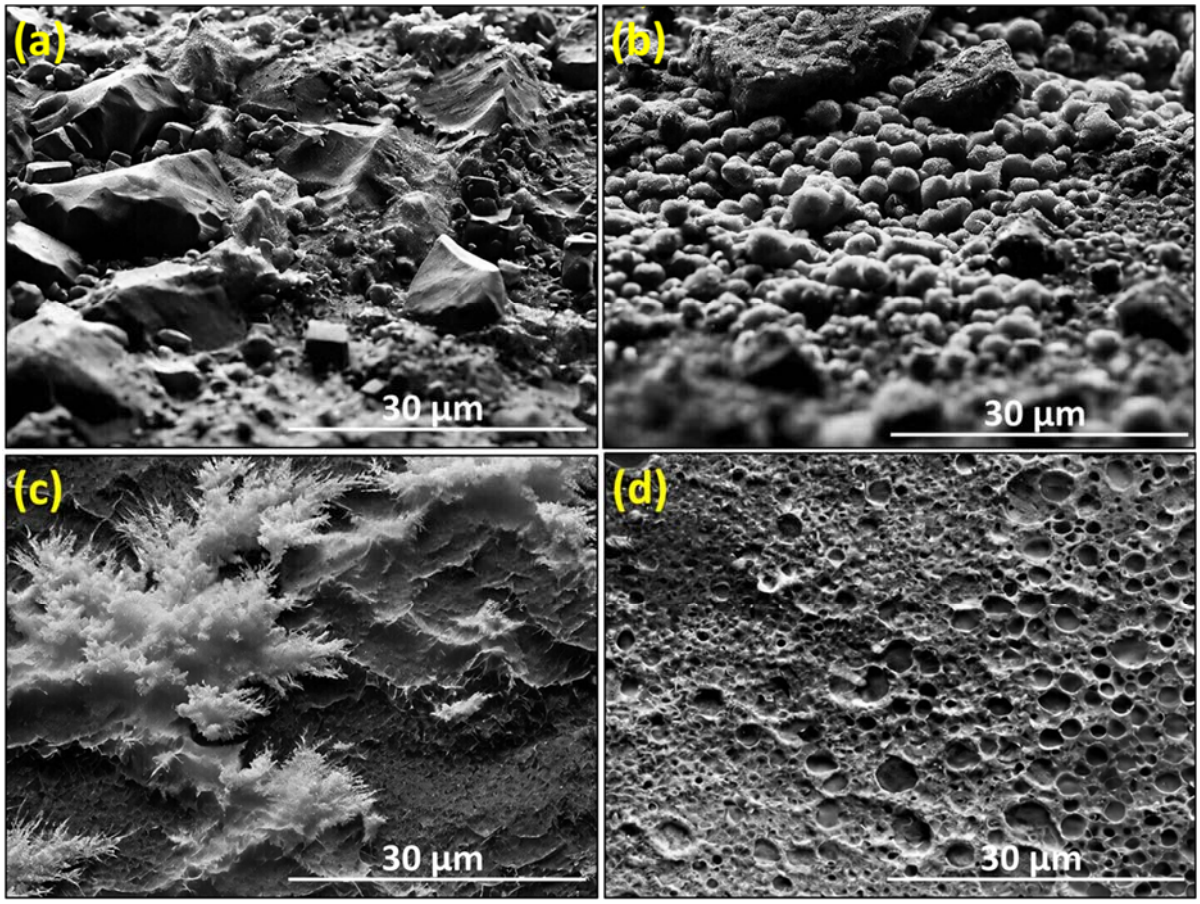

Figure 2. The SEM Micrograph of the sintered composite (ZrO_2-Cr-Ni-Ce-Y) at various temperatures (a) 850°C-950°C, (b)1050°C-1150°C, (c)1250°C, (d)1350°C.

Subsequently, significant changes occurred between 1050 °C and 1150 °C, characterized by smaller stone-shaped structures, reflecting the impact of increased sintering temperature. The kinetics of the sintering process are influenced by temperature. At higher temperatures, sintering occurs more rapidly, leading to accelerated densification and structural changes in the material [17]. At 1250 °C, these stone-shaped structures fused to form layered structures, resembling flowing fluid but maintaining solidity upon closer inspection. The higher temperature promoted additional atom transport and reorganization in the material, which resulted in the fusing of these discrete structures into stratified structures. The smooth, continuous look of these layered formations gave the impression that they were flowing fluid, simulating the fluid-like behavior of molten materials. But upon closer examination, it was clear that these formations were nonetheless solid, meaning that even though they looked fluid, they still had structural coherence and integrity. This phenomenon highlights the dynamic nature of phase changes in designed materials by illuminating the intricate interactions between temperature, material composition, and microstructural evolution throughout the sintering process [18] After the completion of the sintering process at 1350 °C, a layer of silverish white coloration, alongside polar white cotton-shaped structures, emerged, indicating the fusion of cerium and yttrium with the boundaries of the ZrO_2-Cr-Ni matrix. Furthermore, the micrograph developed at 1350 °C highlighted the formation of strong metallurgical bonds between grains, resulting in a sudden decrease in porosity and an increase in the degree of dissolution. This densification process, occurring relatively late, led to the formation of compactly packed microstructures within the metal-composite.

3.2. Density

 doi:10.20944/preprints202409.0398.v1

Figure 3 illustrates the impact of sintering temperature on the density and porosity of sintered compacts. It is evident that both densities increase significantly with rising sintering temperatures during the initial phase of the sintering process. Solid-phase sintering occurs at 850°C and 1350°C, temperatures below the melting point of Ce (796°C). During this phase, enhanced atomic diffusion improves particle contact, reduces porosity, and facilitates the formation and growth of sintering necks, thereby increasing the both densities. When the temperature surpasses Ce melting point (796°C), a bridged Ce network forms as the liquid Ce phase bonds and links different composite particles. Porosity is inversely proportional to density, decreasing as density increases. Figure 3 demonstrates the relationship between porosity and sintering temperature. This reduction occurs because liquid-phase Ce fill the pores between ZrO_2-Cr-Ni grains. Before sintering, many pores are located at particle contact points and around grains. At 850°C, the Ce liquid phases rearrange to fill the pores, further reducing porosity. However, from 825°C to 1350°C, porosity values rise significantly due to rapid diffusion of Ce into ZrO_2-Cr-Ni composite, leading to large pores (swelling) [19].

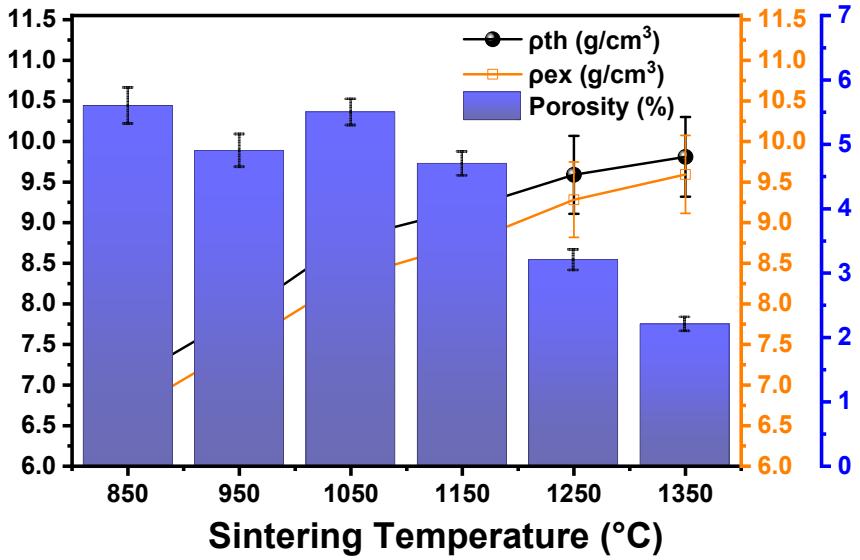

Figure 3. Theoretical density, sintered density, and porosity of ZrO_2-Cr-Ni-Ce-Y composites at various sintering temperature.

3.3. Hardness

Figure 4 shows the hardness versus sintering temperature graph. The data obtained at the temperature range of 850-1350°C was tested using a Vickers hardness tester. This Vickers hardness value closely matched the estimated hardness. Figure 4 revels that observed that with an increase in sintering temperature, the hardness of the ZrO_2-Cr-Ni-Ce-Y metal composite also increases. However, within the sintering temperature of 1150°C, a slight decrease or stabilization in hardness was observed. This decrease or lack of change in hardness values can be attributed to the densification of cerium and yttrium within the lattices of the ZrO_2-Cr-Ni metal composite [20] . During doping of non-metallic and metallic elements stable the hardness occurred due to the reinforcement provided by the doped material to matrixes of metal-composite which would require high amount of energy for complete densification to obtain a homogenous mixed sample. Moreover, cerium and yttrium addition provide a significant reinforcement to the ZrO_2-Cr-Ni metal-composite, which require an extra amount of latent energy during sintering process for full densification. The addition of cerium and yttrium to the ZrO2-Cr-Ni matrix can lead to solid solution strengthening, wherein the atoms of the added elements occupy interstitial or substitutional positions within the crystal lattice, effectively impeding the movement of dislocations and increasing the material hardness [21]. It would also be observed from figure 2 (b), In the sintering temperature range of 1050 °C-1150 °C occurrence of smaller stone-shaped structures was observed as compared from figure 2 (a) which was bigger. From

 doi:10.20944/preprints202409.0398.v1

this instance, the assumptions or valid proof reasons which were mentioned above is clearly a meaningful explanation for this experiment. The hardness was increasing with the sintering temperature. Increased the sintering temperatures facilitate grain growth within the material, resulting in larger crystal structures. the larger crystal structures formed at higher sintering temperatures contribute to the material's increased hardness by reducing grain boundary area, enhancing dislocation interaction, and promoting strain hardening. These mechanisms collectively improve the material resistance to deformation and make it harder [22].

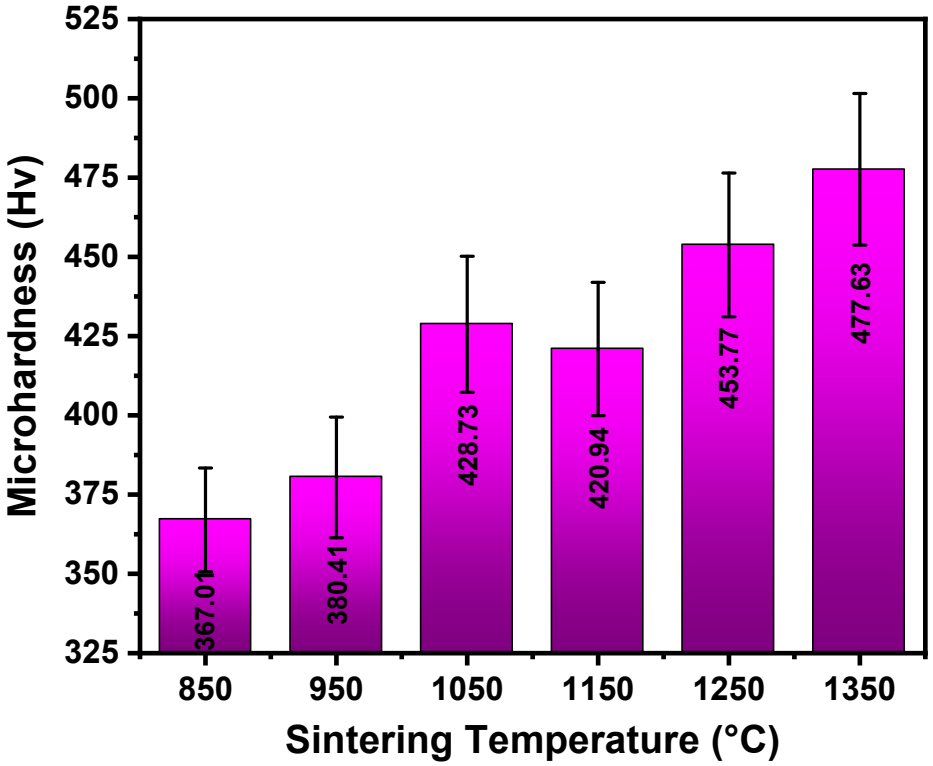

Figure 4. Represents the microhardness of the fabricated composite (ZrO_2-Cr-Ni-Ce-Y) sintered at various sintering temperatures.

3.4. Flexural Strength

Figure 5 illustrates the variation of sintered (Ce and Y mixed) at different sintering temperatures of 850 °C, 950 °C, 1050 °C, 1150 °C, 1250 °C and 1350 °C along with porosity percentage. It was observed, the addition of cerium and yttrium in ZrO_2-Cr-Ni metal-composite increases the Flexural strength which attain a maximum value of 964.32 MPa at 1350 °C °C. Also, it was seen that at this value the rate of porosity also decreases quite swiftly. From Figure 3 it would be observed, at 1050 °C the percentage of porosity advances abruptly, however the value of Flexural strength didn't decline during this phase in comparison with value at 950 °C sintering temperature. The best viable reason sustains, the densification of individual molecular structure of ZrO_2, Cr, Ni, Ce and Y. This might involve the utilization of latent heat which would breaks molecular bonds existence in between the ZrO_2 atoms. Also, the formation of different solid solution formed during compaction and sintering process i.e., Y_2O_3 and CeO_2. These self-evolving compounds create a disturbance in the stacking of microstructures as per designed boundary conditions. But suddenly at 1150 °C-1186 °C the porosity percentage increases for the (Ce and Y doped) and resembles a value of 27%. This sudden increment in the rates of porosities creates the next level of research in this current experiment. The most prominent reason behind the abrupt nature of level of porosities could be explained through understanding the concept of atomic radii of individual element used in this metal-composites (Zr, Cr, Ni, Ce and Y). The atomic radius of Zr-0.160 nm, Cr-0.130 nm, Ni-0.124 nm, Ce-1.82 Å and Y-2.27 Å. It was observed that Zr, Cr, and Ni were having almost equal range of radius values. When these

 doi:10.20944/preprints202409.0398.v1

all elements were mixed homogenously and prepared for compaction and sintering process, the occurrence of a gap existed at their inter-atomic spaces. These gaps were existed in the values, close enough to cerium and yttrium atomic radii. The atomic radius of cerium and yttrium were lesser than ZrO_2, Cr and Ni elements, which made these doping agents as perfect ingredients to fill the gaps of metal-composite during compaction and sintering process. The atoms of cerium and yttrium densifies completely into ZrO_2-Cr-Ni matrix during sintering process with an extra amount of latent energy in the same range of sintering temperature i.e., at 1050 ^{O}C. Afterward, at temperature 1150 °C-1186 °C the sudden increase in porosity percentage with Flexural strength simultaneously. With the propagation of sintering temperatures, the rate of porosity decreases instantly. The addition of yttrium has enhanced the strength of fabricated composite samples. During compaction and sintering process, the doping agents needs some time to densify completely into the metal-composite matrix which require an extra amount of latent energy. This results the abrupt nature of porosity with affecting the mechanical behaviour of the metal-composite [23]. However, the Flexural strength didn't affect as it's always maintained a linear relationship with sintering temperature. But, it was observed in the case of ZrO_2-Cr-Ni, in the range of sintering temperature from 1000 °C -1200 °C the values of flexural strength were much more than 577.70 MPa. From these conclusions it's confirmed that too some extent the flexural strength also affected by doping ZrO_2-Cr-Ni metal-composite with cerium and yttrium in the sintering temperature range of 1000 ^{O}C-1200 ^{O}C. Finally, from all these data and observation it could be concluded too, the doping of cerium and yttrium enhances the mechanical behaviour of the metal-composite (ZrO_2-Cr-Ni) and co-relates the changes occurred in microstructural and phase transformation with the mechanical behaviour of the metal-composite. Several possible reasons would be evolved in the disturbances caused in the abrupt relationship with porosity percentage v/s sintering temperature and flexural strength. May be the addition of iso-propyl alcohol used as a binding agent during compaction process.

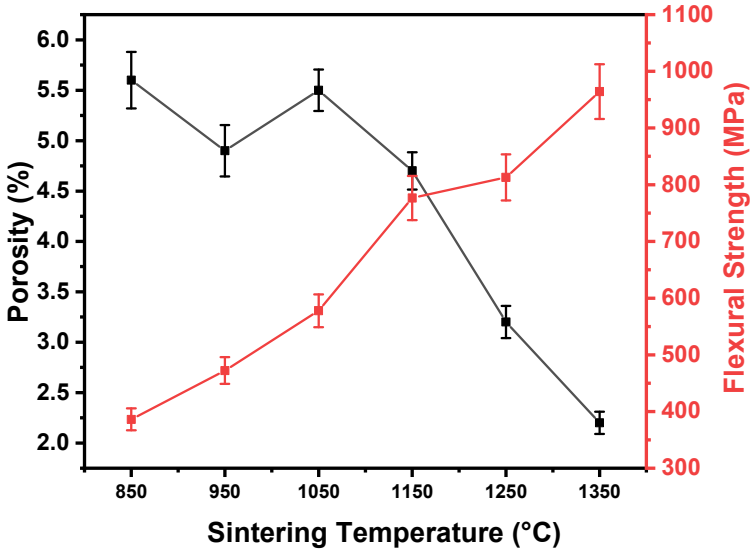

Figure 5. Flexural strength of the sintered ZrO_2-Cr-Ni-Ce-Y composite at various temperatures and different levels of porosity.

5. Conclusions

The study provides a comprehensive analysis of the microstructural evolution, density, hardness, and flexural strength of a sintered composite consisting of ZrO2-Cr-Ni-Ce-Y across various sintering temperatures. The key findings can be summarized as follows:

- SEM micrographs show a homogeneous distribution of ZrO2, Cr, Ni, Ce, and Y phases, indicating effective fabrication. At lower sintering temperatures (850°C to 950°C), the microstructure features stone-shaped structures due to slow fusion rates, which evolve into smaller forms between 1050°C and 1150°C.

 doi:10.20944/preprints202409.0398.v1

- The composite microstructure evolved from coarse, stone-shaped structures at lower temperatures to finer, layered formations at higher temperatures, culminating in a dense, compact structure at 1350°C.
- Density increased with temperature, primarily due to pore filling by liquid Ce phase, but was counteracted by pore formation from Ce diffusion at higher temperatures.
- Hardness generally improved with temperature, influenced by solid solution strengthening and grain refinement.
- Flexural strength steadily increased with temperature, reaching a peak at 1350°C, demonstrating the composite's potential for high-performance applications.
- The addition of Ce and Y played a crucial role in enhancing mechanical properties through solid solution strengthening and pore filling.

Author Contributions: BCS, DKR - conducted experimental tests on composites and performed data processing; NJ, VS and AV - helped with the collection of data from the scientific literature review, organized the results obtained from the scientific community, and manuscript writing; DMG, KR and DGP - contributed to result interpretation and the discussion of the selected results. All authors have read and agreed to the published version of the manuscript.

Funding: This research received no external funding.

Data Availability Statement: The data presented in this study are available within the article.

Conflicts of Interest: The authors declare no conflicts of interest.

References

1. J. Cho, J. Li, H. Wang, Q. Li, Z. Fan, A.K. Mukherjee, W. Rheinheimer, H. Wang, and X. Zhang, Mater Res Lett **7**, 194-202 (2019).
2. J. Li, Z. Hao, Y. Shu, and J. He, Journal of Materials Research and Technology **9**, 14792-14798 (2020).
3. J. Tian, D. Zhang, Y. Chen, G. Zhang, and J. Sun, Vacuum **170**, 108779-108788 (2019).
4. Y. Wu, Q. Yan, and X. Zhang, Int J Refract Metals Hard Mater **86**, 105093-105103 (2020).
5. B. Zhu, M. Duke, L. Dumée, A. Merenda, E. des Ligneris, L. Kong, P. Hodgson, and S. Gray, Membranes (Basel) **8**, 83-110 (2018).
6. Y. Chen, X. Hou, M. Liao, W. Dai, Z. Wang, C. Yan, H. Li, C.-T. Lin, N. Jiang, and J. Yu, Chemical Engineering Journal **381**, 122690-122697 (2020).
7. Zhang, Yang, Li, and Wu, Metals (Basel) **9**, 961-976 (2019).
8. T. Sun, Z. Zhao, Z. Liang, J. Liu, W. Shi, and F. Cui, Appl Surf Sci **416**, 656-665 (2017).
9. S.-Y. Jian, Y.-C. Tzeng, M.-D. Ger, K.-L. Chang, G.-N. Shi, W.-H. Huang, C.-Y. Chen, and C.-C. Wu, Mater Des **192**, 108707-108721 (2020).
10. Y. Ikoma, T. Toyota, Y. Ejiri, K. Saito, Q. Guo, and Z. Horita, J Mater Sci **51**, 138-143 (2016).
11. R. Kumar, E. Jordan, M. Gell, J. Roth, C. Jiang, J. Wang, and S. Rommel, Surf Coat Technol **327**, 126-138 (2017).
12. X. Deng, Y. Wang, Y. Chen, Z. Cui, and C. Shi, J Solid State Chem **275**, 206-209 (2019).
13. Y. Wang, B. Gao, S. Li, B. Jin, Q. Yue, and Z. Wang, Chemosphere **218**, 974-983 (2019).
14. J. Zhou, Y. Yang, Y. Yang, D.S. Kim, A. Yuan, X. Tian, C. Ophus, F. Sun, A.K. Schmid, M. Nathanson, H. Heinz, Q. An, H. Zeng, P. Ercius, and J. Miao, Nature **570**, 500-503 (2019).
15. R.I. Shakirzyanov, N.O. Volodina, A.L. Kozlovskiy, M. V. Zdorovets, D.I. Shlimas, D.B. Borgekov, and Y.A. Garanin, Journal of Composites Science **7**, 411-430 (2023).
16. T.S. Natarajan, V. Mozhiarasi, and R.J. Tayade, Photochem **1**, 371-410 (2021).
17. G.R. Xu, J.L. Zou, and G.B. Li, J Hazard Mater **150**, 394-400 (2008).
18. S.A. McDonald, C. Holzner, E.M. Lauridsen, P. Reischig, A.P. Merkle, and P.J. Withers, Sci Rep **7**, 5251-5262 (2017).
19. L. Wang, B. Ma, X. Ren, C. Yu, J. Tian, C. Liu, C. Deng, C. Hu, Z. Liu, J. Yu, and Z. Jiang, Mater Today Commun **30**, 103032-103042 (2022).
20. A.M. Khalil, A. V. Pozdniakov, A.N. Solonin, T.S. Mahmoud, M. Alshah, and A.O. Mosleh, Materials **16**, 5477-5490 (2023).
21. L. CHANG, B. JIA, S. LI, X. ZHU, R. FENG, and X. SHANG, Journal of Rare Earths **35**, 1029-1034 (2017).
22. Z. Shen, Y. Zhen, K. Wang, and J. Li, Journal of the American Ceramic Society **92**, 1748-1752 (2009).
23. M.A. Almomani, A.M. Shatnawi, and M.K. Alrashdan, Adv Mat Res **1064**, 32-37 (2014).

 doi:10.20944/preprints202409.0398.v1